Article

J. Mex. Chem. Soc. **2013**, *57(2),* 73-79

ISSN 1870-249X

Hydrothermal Synthesis of Mesoporous Silica MCM-41 Using Commercial Sodium Silicate

Héctor Iván Meléndez-Ortiz,* Alfonso Mercado-Silva, Luis Alfonso García-Cerda, Griselda Castruita, and Yibran Argenis Perera-Mercado

Centro de Investigación en Química Aplicada (CIQA). Boulevard Enrique Reyna Hermosillo #140, C.P. 25294; Saltillo, Coahuila, México. ivan_melendez380@hotmail.com

Received September 5, 2012; accepted April 4, 2013

Abstract. In this work, ordered mesoporous silica MCM-41 was prepared by hydrothermal synthesis using industrial-grade sodium silicate (Na_2SiO_3) as silica source, hexadecyltrimethyl-ammonium bromide (CTAB) as template agent and ethyl acetate as pH regulator. The influence of CTAB/SiO_2 molar ratio, reaction time, aging temperature, and co-surfactant type on the structural and morphological properties of the obtained silica was studied. The products were characterized by X-ray diffraction (XRD), scanning electron microscopy (SEM), transmission electron microscopy (TEM) and nitrogen adsorption-desorption isotherms. Ordered mesoporous MCM-41 silica was obtained at 80 °C by using a range of CTAB/SiO_2 molar ratio from 0.35 to 0.71 and reaction times up to 72 h and isopropanol (*i*-PrOH) as co-surfactant.
Key words: Mesoporous silica, MCM-41, sodium silicate, hydrothermal synthesis, X-rays.

Resumen. En este trabajo se preparó sílice mesoporosa MCM-41 hidrotermalmente usando silicato de sodio (Na_2SiO_3) grado industrial como fuente de sílice, bromuro de hexadeciltrimetilamonio (CTAB) como surfactante y acetato de etilo como regulador de pH. Se estudió la influencia de la relación molar CTAB/SiO_2, tiempo de reacción, temperatura y tipo de co-surfactante sobre las propiedades estructurales y morfológicas de la sílice mesoporosa. Los productos fueron caracterizados mediante difracción de rayos X, microscopía electrónica de barrido, microscopia electrónica de transmisión y adsorción-desorción de nitrógeno. Sílice MCM-41 ordenada estructuralmente fue obtenida a 80 °C usando una relación molar CTAB/SiO_2 en un rango de 0.35 a 0.71 y tiempos de reacción mayores a 72 h con isopropanol (*i*-PrOH) como co-surfactante.
Palabras clave: Sílice mesoporosa, MCM-41, silicato de sodio, síntesis hidrotermal, rayos X.

Introduction

Since the discovery of ordered mesoporous silica materials [1, 2], different works for the preparation of this kind of materials using cationic surfactants as a template have been published [3-5]. Usually, their preparation consists in the formation of micelles in aqueous solution, followed by the polymerization of an inorganic source and the removal of surfactants from the pores of the material [5].

MCM-41 has a hexagonal arrangement of one-dimensional mesopores with diameters ranging from 2 to 10 nm [2]. The homogeneity of the pores, high surface area, and good thermal stability, which make them an attractive molecular sieve for applications in catalysis, sorption of large organic molecules, chromatographic separations, as well as host for quantum confinement of guest molecules [6].

The porosity and morphology of MCM-41 are determined by different processing parameters as the type of surfactant template and silica source, composition of starting materials, pH, temperature, aging time, additives, and solvents [7]. Soluble silicate compounds such as tetraethylorthosilicate (TEOS) [8, 9] and sodium silicate (Na_2SiO_3) have been mainly used as silica sources for the synthesis of mesoporous silica [10]. TEOS can be hydrolyzed to obtain silanol groups while a solution of Na_2SiO_3 already offers these groups, and their amount depends on the precondensation degree. With a higher degree of silica precondensation, the possibilities to obtain well-ordered materials are lower. During MCM-41 preparation, the rate of silanol condensation depends not only on the temperature and pH of the reaction medium, but also on the presence of additional ions and the silicate concentration. One of the advantages in employing Na_2SiO_3 as the silica source is its cost; however, the obtained MCM-41 is structurally less stable than the equivalent analogues prepared from TEOS in the absence of sodium. This implies that the small amount of sodium that inevitably is incorporated into the framework of the mesostructure may collapse the framework under hydrothermal conditions [11].

Some attempts have been reported to prepare MCM-41 mesoporous silica from Na_2SiO_3 [12-14]. Park [15] reported the preparation of MCM-41 using microwave heating and ethylene glycol as additive. However, poorly crystallized MCM-41 is obtained when ethylene glycol is added at large amounts. Han *et al*. [4] prepared hollow spherical silica with MCM-41 structure using propanol as a co-surfactant. They found that the molar ratio of propanol to CTAB in the starting composition affects the morphology of the mesoporous silica. Mendoza [16] studied the composition and reaction time in the pore ordering and morphology of MCM-41. They found four different morphologies of the product (hexagonal platelets, gyroids, crescent-like or worm-shape particles) by the combination of CTAB, H_2O, and ethyl acetate content of the reaction mixture. Recently, Mody [17] prepared MCM-41 at room temperature using CTAB as a structure directing agent under acidic conditions.

Thus, the aim of this paper was to develop a simple route to obtain mesoporous silica MCM-41 from inexpensive silica source (Na_2SiO_3) and evaluate the effect of some conditions of reaction, such as composition of starting materials, type of co-surfactant, temperature, and aging time on the structural

ordering and morphology of the prepared silicas in order to obtain the optimum conditions of synthesis.

Results and discussion

Influence of temperature

The effect of the hydrothermal temperature on the pore structure ordering of mesoporous MCM-41 silica was studied in order to establish temperature conditions of experiments under the procedure used in this work. Experiments were carried out using a CTAB/SiO_2 molar ratio of 0.71 and *i*-PrOH as co-surfactant and temperatures of 80, 90 and 100 °C. Figure 1 shows the XRD diffractograms of these samples. It is evident that an increase of temperature affects negatively the formation of MCM-41 silica. It can be seen that the characteristic diffraction peaks of the planes (100), (110), and (200) appeared at 2.41, 4.14 and 4.8° of 2θ respectively for sample prepared at 80 ºC. Nevertheless, further increase of the hydrothermal temperature resulted in a poor structure ordered silica and even at 100 ºC it can be seen that silica was not formed. This could be explained because of at higher temperature NH_4OH and H_2O started to evaporate due to the system containing solution was not completely hermetic and then the initial composition of mix could not be kept. However, this result indicates that ordered structure MCM-41 silica can be obtained using relative low hydrothermal temperature and it would be an advantage in the large-scale production of hexagonal mesoporous MCM-41 silica [18] and then further experiments were carried out at 80 °C (Fig. 1).

Influence of CTAB/SiO_2 molar ratio

Figure 2 shows the XRD patterns for calcined MCM-41 silica obtained at different CTAB/SiO_2 molar ratios. The MCM-41 samples synthesized in a range from 0.53 to 0.71 show the corresponding peaks for the planes (100), (110) and (200) located at 2.3, 4.1 and 4.7° of 2θ respectively (Table 1). Both, decreasing or increasing out of this range resulted in a decrease of the pore mesostructure ordering due to the disturbing of the assembly on MCM-41 structure during process of synthesis. By comparing XRD diffractograms of the silica samples synthesized at CTAB/SiO_2 molar ratio of 0.53 and 0.71, it could be seen that the first one has a better quality due to the characteristic peak of the plane (100) is more intense and sharp. In addition, the peaks of the planes (110) and (200) (attributed to the 2D hexagonal structure of MCM-41 silica) are more defined. On the other hand, as the amount of SiO_2 is increased, the three peaks are shifted to lower 2θ values. This behavior could be attributed to a thicker pore wall as can be seen in the values of Table 2. In the case for MCM-41 sample synthesized with CTAB/SiO_2 molar ratio of 0.35, it did not show the signals for the planes (110) and (200). This behavior is due to the increase in the surfactant concentration cause prohibition of unit cell growth and decrease in polymerization of silica resulting in poor hexagonal ordered MCM-41 silica.

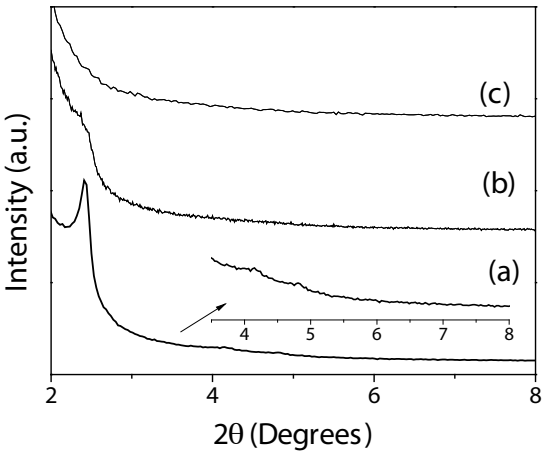

Fig. 1. XRD patterns of MCM-41 silica obtained at different temperatures.

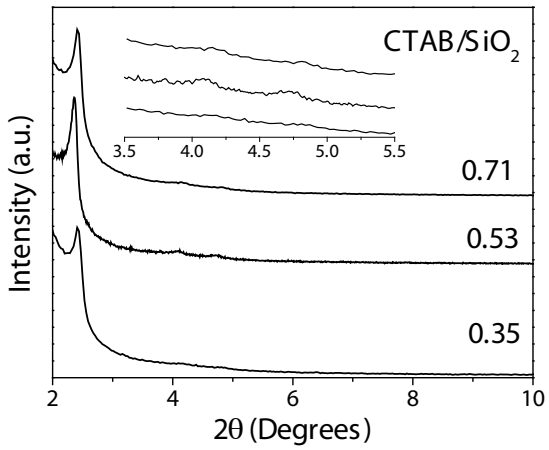

Fig. 2. XRD patterns of MCM-41 silica obtained at different CTAB/SiO_2 molar ratios.

Influence of ethyl acetate hydrolysis reaction time

Figure 3 shows the XRD patterns of MCM-41 silica prepared at different hydrolysis reaction time. Studies were carried out at 80 °C with a CTAB/SiO_2 molar ratio of 0.71 and aging time of 72 h. This figure shows the formation of MCM-41 in all cases. However, when hydrolysis reaction time is increased the pore structure ordering decreases. This behavior is detected by a clear reduction of the intensity of the reflection peaks (110) and (200). This indicated that the pore structure of the sample become more ordered when the ethyl acetate hydrolysis is carried out for 3 h. The reason that ethyl acetate affected the pore structure ordering was that ethyl acetate is a good co-solvent for CTAB and when hydrolysis time increases more ethanol and acetic acid are generated and they could destroy the micellar template and make the pore structure less ordered. This is because of acidification of Na_2SiO_3 solutions yields amorphous silica gels and in more alkaline pH range the required time to

Table 1. The 2θ, d-spacing of plane (100) and unit cell parameter values for MCM-41 silica synthesized at different conditions.

$CTAB/SiO_2$ molar ratio	2θ (100)	2θ (110)	2θ (200)	d_{100} (nm)	Unit cell parameter a_0 (nm)
0.35	2.41	ND	ND	3.66	4.22
0.53	2.36	4.11	4.70	3.73	4.30
0.71	2.41	4.14	4.80	3.66	4.22
Reaction time (h)					
48	2.37	ND	ND	3.72	4.29
72	2.41	4.14	4.8	3.66	4.22
110	2.39	4.09	4.72	3.69	4.26
Aging temperature (°C)					
80	2.41	4.14	4.8	3.66	4.22
Type of					
Co-surfactant					
i-PrOH	2.41	4.14	4.8	3.66	4.22
BuOH	2.20	4.03	4.62	3.99	4.61
Ethyl acetate hydrolysis reaction time (h)					
3	2.31	3.99	4.56	3.81	4.41
5	2.41	4.14	4.8	3.66	4.22
7	2.38	4.06	4.72	3.70	4.28

Table 2. Comparison of some parameters for some MCM-41 obtained at room temperature and different $CTAB/SiO_2$ molar ratios.

$CTAB/SiO_2$ ratio	Total pore volume (cm^3/g)	BET surface area (m^2/g)	BJH average pore diameter (nm)	Wall thickness (nm)
0.53	1.69	1028	2.38	1.92
0.71	1.35	860	2.50	1.72

form gel decreases [19]. Thus, the mixtures prepared at higher hydrolysis reaction time have a lower final pH.

Effect of co-surfactant

It is well-known that use of co-surfactants in the synthesis of mesoporous materials affects important material properties, such as pore diameter, mesostructure order and phase behavior [20]. For this reason, some co-surfactants were proved in order to know how they affect the mesostructure of the MCM-41 silica. Figure 4 shows the XRD diffractogram patterns for MCM-41 samples obtained with two different alcohols: butanol (BuOH) and i-PrOH. From this figure, it can be seen that well-ordered mesoporous MCM-41 silica was obtained with *i*-PrOH. In this case, typical three diffraction peaks were observed for the planes (100), (110), and (200). On the other hand, sample

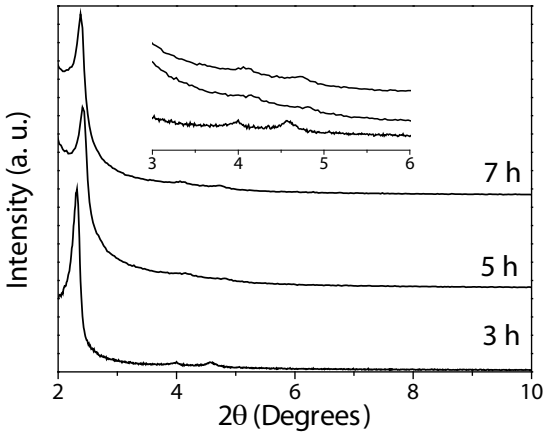

Fig. 3. Dependence of ethyl acetate hydrolysis reaction time on XRD patterns for MCM-41 silica.

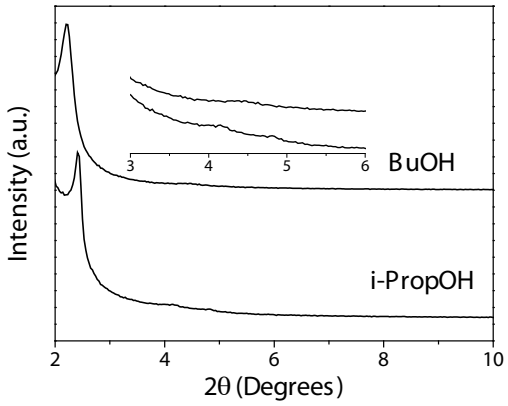

Fig. 4. XRD patterns of MCM-41 silicas obtained with different type of surfactant. $CTAB/SiO_2$ molar ratio of 0.71 and aging temperature and time of 80 °C and 72 h respectively.

synthesized from BuOH showed only a broad peak (plane 100) at low values of 2θ (see Table 1) while the peaks for the (110) and (200) are missing completely as result of a disordered silica structure. This behavior could be explained because when increasing the number of carbon atoms in the chain of co-surfactant the extent of condensation decrease. Thus, the higher condensation rates the better ordered mesoporous silica. Also, MCM-41 sample obtained from BuOH showed the highest d-spacing value (see Table 1). This can be attributed to an increase of the amphiphilic bilayer thickness of the surfactant phase when alcohol chain length increase [20].

Dependence of reaction time

Mesoporous MCM-41 silica was prepared at different intervals of time between 48 and 110 h to explore the optimum reaction synthesis time. The XRD patterns are showed in Figure 5. These samples were obtained at aging temperature of 80 °C and CTAB/SiO_2 molar ratio of 0.71 using *i*-PrOH as co-surfactant. The samples synthesized at 72 and 110 h showed the three characteristic diffraction peaks of the hexagonal-ordered silica MCM-41 while the sample obtained at 48 hours showed only one broad peak due to the plane (100) of a mesostructured hexagonal MCM-41 phase with poor crystallinity [21]. For sample synthesized at 72 and 110 h, the XRD peak positions for the plane (100) shifted slightly to lower 2θ values as the reaction time was increased (see Table 1). The shifting might be associated with a bigger mesopore size [22]. After the addition of silica source, facilitation of hydrolysis and condensation of Na_2SiO_3 with longer stirring results in higher-ordered structure MCM-41 silica.

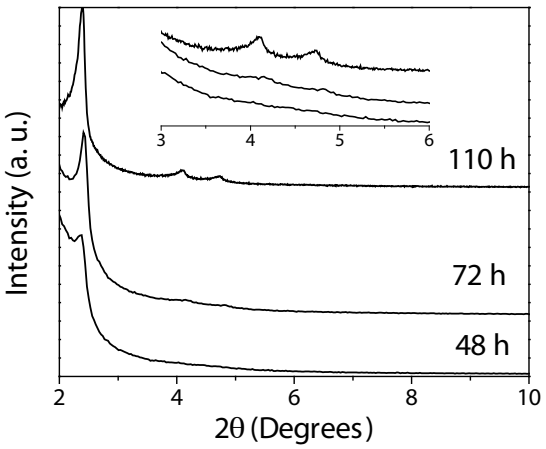

Fig. 5. XRD patterns of MCM-41 silicas synthesized at different aging time.

It is interesting to note that no mesophases are formed during aging process as other authors have reported previously [21, 23, 24]. On the other hand, Mendonza *et al*. [16] reported that with a longer reaction time, the MCM-41 is degraded; they observed a decrease of the intensity of the peak of the plane (100). In our case, a longer reaction time permits to obtain higher ordered mesostructure MCM-41 silica without degradation.

Characterization of MCM-41 silica

Figure 6 shows the nitrogen adsorption isotherms (a) and the pore size distribution (b) for MCM-41 silica synthesized with CTAB/SiO_2 molar ratios of 0.71 and 0.53 during 110 h and using *i*-PrOH as co-surfactant. Both samples showed nitrogen adsorption-desorption isotherms typically of type IV with H1 hysteresis loop [25]. Samples exhibited pronounced steep condensation step for relative pressures 0.6 - 0.9 arising from condensation of nitrogen inside the mesopores and indicating good structural order of MCM-41. The condensation is steep particularly for MCM-41prepared from CTAB/SiO_2 molar ratio of 0.53 as compared to MCM-41 silica synthesized from CTAB/SiO_2 molar ratio of 0.71. Thus, the quality of the product was found to affect the steepness of the condensation steep. This result is in agreement with XRD results described in section 2.2 where the three reflection planes (100), (110) and (200) looked out more intense and defined for the sample prepared from CTAB/SiO_2 molar ratio of 0.53. The specific pore volume, BET surface area, average BJH pore diameter and estimated pore wall thickness deduced from the nitrogen sorption isotherms for these samples are summarized in Table 2. High specific surface area values are obtained for both samples

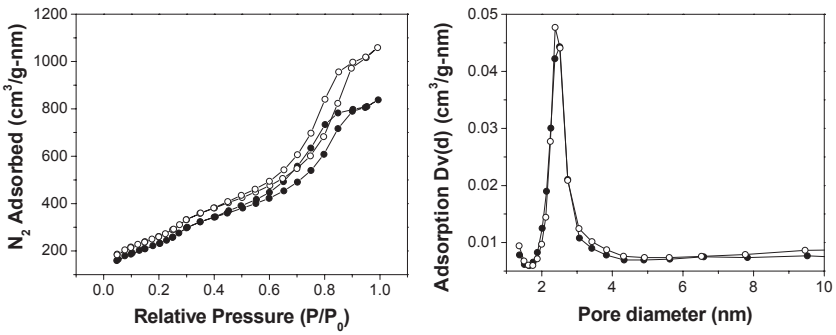

Fig. 6. (a) Nitrogen adsorption isotherms and (b) pore distribution for MCM-41 synthesized at different CTAB/SiO_2 molar ratio: (○) 0.53 and (●) 0.71.

(higher than 850 m^2/g). Also, MCM-41mesoporous molecular sieves exhibited narrow pore size distribution (pore sizes from 2 to 3 nm). The wall thickness values were calculated by the following equation:

$$W_t = a_0 - \text{average pore diameter}$$

The estimated wall thickness values were in the range from 1.72 to1.92 nm and they are agreeing with previous reports [17, 26]. Silica synthesized with a CTAB/SiO_2 molar ratio of 0.53 showed a higher wall thickness and this result agrees with the shift of 2θ value from XRD diffractogram discussed in section 2.2. All these properties make them an attractive molecular sieve for application, such as, catalysis, sorption of organic molecules, chromatographic separations, etc. [6].

Figure 7 displays SEM images of the mesoporous MCM-41 silica obtained at different CTAB/SiO_2 molar ratio. Samples obtained with a CTAB/SiO_2 molar ratio of 0.71 (Fig. 7a) showed a more regular shape by comparing with the MCM-41 sample obtained with a molar ratio of 0.53 (Fig. 7b). The first one, showed a well-defined spherical morphology with particle size range from 300 to 500 nm whereas the other sample exhibited an irregular morphology without defined form and smaller particle size. The structure of various samples of MCM-41 silica was also characterized by TEM. The morphologies and microstructure of the obtained MCM-41 samples are clearly revealed by TEM. Figure 8 shows the images for the MCM-41 silica obtained at 80 °C (a) and 90 °C (b). The MCM-41 sample obtained at 80 °C showed well defined spherical shape with a highly ordered hexagonal long-range array of the channels and streak structural while the sample obtained at 90 ºC did not show any structural arrangement due to its poorly crystalline nature which is in agreement with the results of XRD (see Fig. 1). Finally, SEM and TEM results are in agreement with results described in section 2.6 where samples presented a H1 hysteresis loop which is associated with porous materials of uniform spheres in regular array and with narrow pore size distribution [25].

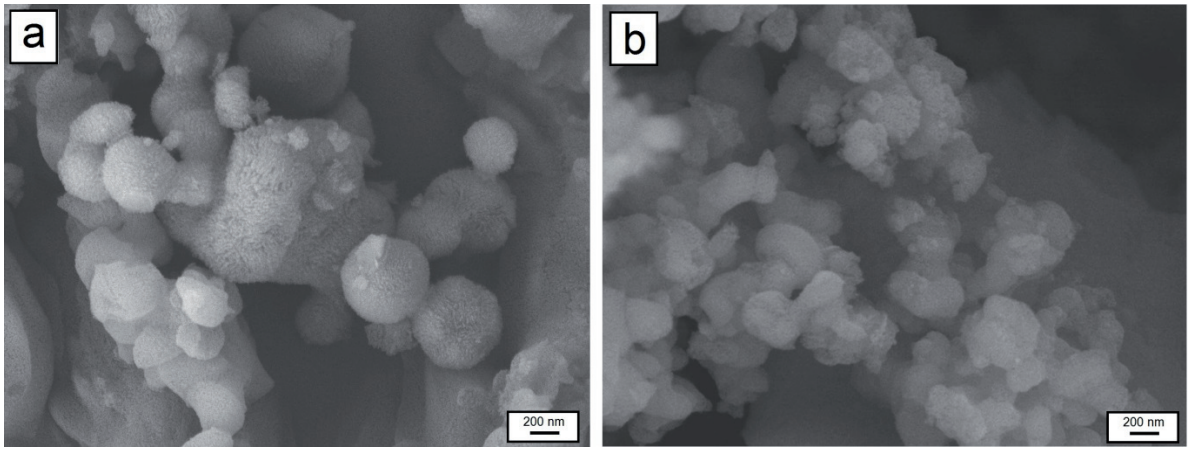

Fig. 7. SEM micrographs for MCM-41 synthesized at different CTAB/SiO_2 molar ratio: (a) 0.71 and (b) 0.53. Magnification of 30,000.

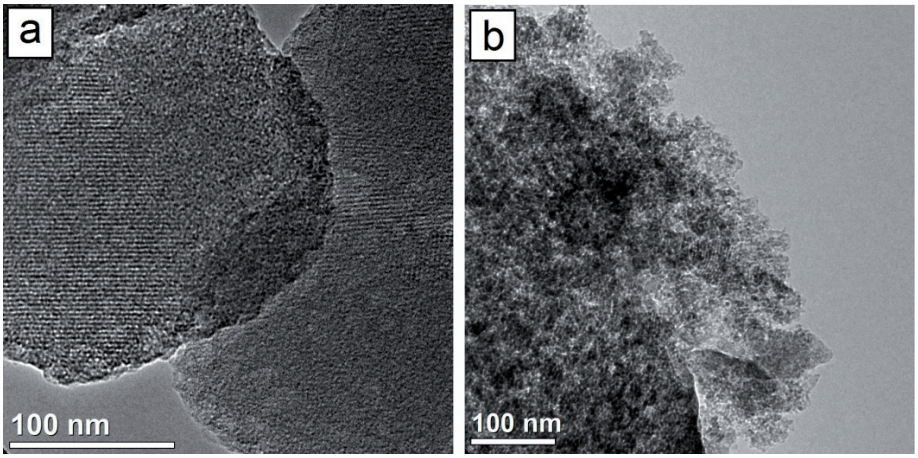

Fig. 8. TEM micrographs for MCM-41 synthesized at different reaction conditions: (a) 80 °C and (b) 90 °C.

Experimental

Reagents

Hexadecyltrimethyl-ammonium bromide (CTAB) (>98%, cationic surfactant), ethyl acetate anhydrous (99.8%, pH regulator), butanol (99.8% co-surfactant) and 2-propanol anhydrous (99.5%, co-surfactant) were purchased from Sigma Aldrich. Sodium silicate (Na_2SiO_3) with a molar ratio of SiO_2/Na_2O = 3.2 (silica source) was obtained from PROQUISA. Deionized water was obtained from a system of two ionic interchange columns (Cole-Parmer Instruments).

Preparation of mesoporous MCM-41 silica

In a typical procedure, a desired amount of CTAB was mixed with 7 mL of 2-propanol (*i*-PrOH) and 100 mL of deionized water until total dissolution, separately, 3 g of Na_2SiO_3 solution were dissolved in 33 mL of deionized water and then both solutions were cooled at 4 °C. After that, Na_2SiO_3 solution was slowly added dropwise to CTAB/i-PrOH solution under vigorous stirring. Subsequently, the resulting mixture was sonicated during 2 h and then 10 mL of ethyl acetate were added, and the solution was sonicated during 5 min again. This solution was kept at 30 °C under magnetic stirring during 5 h in order to promote hydrolysis of ethyl acetate. Finally, the solution was kept at 80 °C for 72 h. The solid obtained was separated by filtration and washing with deionized water and dried at room temperature. The surfactant was removed by calcining at 540 °C for 5 h in air at heating rate of 1 °C/min.

Characterization

X-ray diffraction (XRD) patterns were obtained using a Siemens D-5000 using Cu radiation (λ = 0.15406 nm) operated a 25 mA and 35 kV. Scanning electron microscopy (SEM) images were obtained on a JEOL JSM-7401F operated at 5 kV, and transmission electron microscopy (TEM) was performance on TITAN 80 operated at 300 kV. Finally, nitrogen adsorption-desorption measurements were obtained using a Quantachrome Autosorb-1 analyzer. For this case, MCM-41 silica samples were first degassed for several h at 300 °C. The measurements were carried out a –196 °C. The specific surface area and pore size distribution were determined by the BJH method.

Conclusions

Ordered mesoporous MCM-41 silica was obtained hydrothermally under the reaction conditions reported in this work without formation of mesophases during aging process. The optimum parameters of synthesis were: $CTAB/SiO_2$ molar ratio from 0.53 to 0.71, reaction time and temperature of 110 h and 80 °C respectively. *i*-PrOH resulted be the best co-surfactant in this case. Also, a short ethyl acetate hydrolysis reaction time (3 h) is preferred to obtain high quality MCM-41 silica. Mesoporous silica MCM-41 synthesized under these reaction conditions showed a well-ordered hexagonal array with spherical morphology and particle sizes of 200 to 500 nm. Mesoporous silica MCM-41 could have potential applications in drug delivery systems, catalysis and sorption of organic molecules due to the high specific surface area.

Acknowledgments

This work was funded by CONACYT - México (Fondo SENER-Hidrocarburos) under grant no. 127499. The authors are grateful to J.A. Cepeda and H. Saade for their technical assistance in the SEM micrographs and N_2 adsorption–desorption studies, respectively.

References

1. Kresge, C. T.; Leonowicz, M. E.; Roth, W. J.; Vartuli, J. C.; Beck, J. S. *Nature* **1992**, *359*, 710-712.
2. Beck, J. S.; Vartuli, J. C.; Roth, W. J.; Leonowicz, M. E.; Kresge, C. T.; Schmitt, K. D.; Chu, C. T. W.; Olson, D. H.; Sheppard, E. W.; McCullen, S. B.; Higgins, J. B.; Schlenker, J. L. *J. Am. Chem. Soc.* **1992**, *114*, 10834-10843.
3. Chen, Y.; Shi, X.; Han, B.; Qin, H.; Li, Z.; Lu, Y.; Wang, J.; Kong, Y. *J. Nanosci. Nanotechnol*. **2012**, *12*, 7239-7249.
4. Han, S.; Hou, W.; Li, Z. *Colloid Polym. Sci*. **2004**, *282*, 1286-1291.
5. Wu, Y.; Zhang, Y.; Cheng, J.; Li, Z.; Wang, H.; Sun, Q.; Han, B.; Kong, Y. *Micro. Meso. Mater*. **2012**, *162*, 51-59.
6. Kato, M.; Shigeno, T.; Kimura, T.; Kuroda, K. *Chem. Mater*. **2005**, *17*, 6416-6421.
7. Kierys, A.; Buda, W.; Goworek, J. *J. Porous Mater*. **2010**, *17*, 669-676.
8. Yoo, W. C.; Stein, A. *Chem. Mater*. **2011**, *23*, 1761-1767.
9. Jomekian, A.; Mansoori, S. A. A.; Bazooyar, B.; Moradian, A. *J. Porous Mater*. **2012**, *19*, 979-988.
10. Inayat, A.; Kunhnt, A.; Schwieger, W.; Einicke, W. D.; Kullman, J.; Enke, D. *J. Porous Mater*. **2011**, *18*, 767-777.
11. Pauly, T. R.; Petkov, V.; Liu, Y.; Billinge, S. J. L.; Pinnavaia, T. *J. Am. Chem. Soc*. **2002**, *124*, 97-103.
12. Wang, R.; Han, S.; Hou, W.; Sun, L.; Zhao, J.; Wang, Y. *J. Phys. Chem. C* **2007**, *111*, 10955-10958.
13. Jiang, T.; Lu, L.; Yang, X.; Zhao, Q.; Tao, T.; Yin, H.; Chen, K. *J. Porous Mater*. **2008**, *15*, 67-63.
14. Vasudevan, M.; Sakaria, P. L.; Bhatt, A. S.; Mody, H. M.; Bajaj, H. C. *Ind. Eng. Chem. Res*. **2011**, *50*, 11432-11439.
15. Park, S. E.; Kim, D. S.; Chang, J. S.; Kim, W. Y. *Catal. Today* **1998**, *44*, 301-308.
16. Mendonza, A. M.; Warzywoda, J.; Sacco, A. *J. Porous Mater*. **2006**, *13*, 37-47.
17. Mody, H. M.; Kannan, S.; Bajaj, H. C.; Manu, V.; Jasra, R. V.; *J. Porous Mater*. **2008**, *15*, 571-579.
18. Diaz, I.; Perez-Pariente, J.; Terasaki, O. *J. Mater. Chem*. **2004**, *14*, 48-53.
19. Liu, S.; Cool, P.; Collart, O.; Van Der Voort, P.; Vansant, E. F.; Lebedev, O. I.; Van Tendeloo, G.; Jiang, M. *J. Phys. Chem. B* **2003**, *107*, 10405-10411.
20. Xu, J.; Luan, Z.; He, H.; Zhou, W.; Kevan, L. *Chem. Mater*. **1998**, *10*, 3690-3698.
21. Han, S.; Xu, J.; Hou, W.; Yu, X.; Wang, Y. *J Phys. Chem. B* **2004**, *108*, 15043-15048.

22. Gaydhankar, T. R.; Samuel, V.; Jha, R. K.; Kumar, R.; Joshi, P. N. *Mater. Res. Bull*. **2007**, *42*, 1473-1484.
23. Kleitz, F.; Blanchard, J.; Zibrowius, B.; Schüth, F. *Langmuir* **2002**, *18*, 4963-4971.
24. Iler, R. K. *The Chemistry of Silica*. Wiley, New York, **1979**.
25. Sing, K. S. W.; Everett, D. H.; Haul, R. A. W.; Moscon, L.; Picrotti, R. A.; Rouquerol, J.; Siemieniewska, T. *Pure Appl. Chem*. **1985**, *57*, 603-619.
26. Vetrivel, S.; Chen, C. T.; Kao, H. M. *New J. Chem.* **2010**, *34*, 2109-2112.